

# The Karavanke Granitic Belt (Slovenia) : a bimodal Triassic alkaline plutonic complex

Autor(en): **Bole, Meta / Dolenc, Tadej / Zupani, Nina**

Objekttyp: **Article**

Zeitschrift: **Schweizerische mineralogische und petrographische Mitteilungen  
= Bulletin suisse de minéralogie et pétrographie**

Band (Jahr): **81 (2001)**

Heft 1

PDF erstellt am: **21.07.2024**

Persistenter Link: <https://doi.org/10.5169/seals-61678>

## **Nutzungsbedingungen**

Die ETH-Bibliothek ist Anbieterin der digitalisierten Zeitschriften. Sie besitzt keine Urheberrechte an den Inhalten der Zeitschriften. Die Rechte liegen in der Regel bei den Herausgebern.

Die auf der Plattform e-periodica veröffentlichten Dokumente stehen für nicht-kommerzielle Zwecke in Lehre und Forschung sowie für die private Nutzung frei zur Verfügung. Einzelne Dateien oder Ausdrucke aus diesem Angebot können zusammen mit diesen Nutzungsbedingungen und den korrekten Herkunftsbezeichnungen weitergegeben werden.

Das Veröffentlichen von Bildern in Print- und Online-Publikationen ist nur mit vorheriger Genehmigung der Rechteinhaber erlaubt. Die systematische Speicherung von Teilen des elektronischen Angebots auf anderen Servern bedarf ebenfalls des schriftlichen Einverständnisses der Rechteinhaber.

## **Haftungsausschluss**

Alle Angaben erfolgen ohne Gewähr für Vollständigkeit oder Richtigkeit. Es wird keine Haftung übernommen für Schäden durch die Verwendung von Informationen aus diesem Online-Angebot oder durch das Fehlen von Informationen. Dies gilt auch für Inhalte Dritter, die über dieses Angebot zugänglich sind.

# The Karavanke Granitic Belt (Slovenia) – a bimodal Triassic alkaline plutonic complex

by Meta Bole<sup>1</sup>, Tadej Dolenc<sup>1</sup>, Nina Zupančič<sup>1</sup> and Breda Činč-Juhant<sup>2</sup>

## Abstract

The rocks of the Karavanke Granitic Belt belong to a bimodal magmatic association consisting of predominant syenogranite and syenite and contemporaneous mafic and intermediate rocks of alkaline character. Mafic rocks (gabbro, monzogabbro) represent about 20% of the whole massif, and range in size from decimetric microgranular enclaves to large decametric bodies. The intermediate rock types (monzodiorite, monzonite) show field, textural and chemical features suggesting that they have formed as a result of the interaction between felsic and mafic magmas. The porphyry syenite with rapakivi texture, which occurs in close spatial association with mafic enclaves, is interpreted as a piece of evidence for such interaction.

Although the rocks represent a continuous series, only minor part of the mafic rocks on one hand and acid rocks on the other hand could be reasonably presented as the product of crystal fractionation. Geochemical features suggest that the majority of the rock types were affected by the interaction of felsic and mafic magmas.

Geochemical character and age of the Karavanke Granitic Belt suggest its pertinence to the alkaline Western Mediterranean Magmatic Province (BONIN et al., 1987) of late Permian to Triassic age.

*Keywords:* alkali granite, mafic enclaves, magma mixing, rapakivi, Karavanke igneous zone.

## 1. Introduction

The intrusive magmatic rocks of the Karavanke Granitic Belt (Slovenia) represent a heterogeneous massif, consisting of predominant syenogranite and syenite with contemporaneous mafic and intermediate rocks of alkaline character. Dikes of porphyry syenite with K-feldspar rimmed by plagioclase (e.g. rapakivi texture) cut large mafic bodies. The area has been investigated by several authors (EXNER, 1971, 1976; FANINGER, 1976; MIOČ, 1983), who mostly described different types of rocks as differentiates of the same parental magma, which is unlikely due to the volume ratio of mafic to felsic rocks.

The association of mafic enclaves in granitic rocks are not uncommon. Different types of enclaves in intrusive bodies have been the object of many studies and were recently reviewed by DIDIER and BARBARIN (1991; and references

therein). Enclaves have been interpreted as re-worked xenoliths, restites, autoliths, disrupted fine-grained borders of the wall of the magma chamber, or blobs of mantle derived magma that intrude felsic, evolved magma. Among these types of enclaves, the “mafic microgranular enclaves” (MME) are generally considered as evidence for magma mixing, as the magma mixing model fits best with most of the main features of mafic microgranular enclaves (BONIN, 1991).

According to many authors, the formation of intermediate rocks as well as the rapakivi texture may be assigned to the interaction of mafic and felsic magmas (FOURCADE and ALLEGRE, 1981; HIBBARD, 1981; REID et al., 1983; BUSSY, 1990; CASTRO et al., 1990; DIDIER and BARBARIN, 1991 and references therein; EKLUND et al., 1994; SALONSAARI and HAAPALA, 1994; RÄMÖ and HAAPALA, 1995 and references therein; BELLINI et al., 1996; CHAPPELL, 1996).

<sup>1</sup> University of Ljubljana, Faculty of Natural Sciences and Engineering, Department of Geology, Aškerčeva 12, SI-1000 Ljubljana, Slovenia. <meta.dobnikar@ntfgeo.uni-lj.si>

<sup>2</sup> Slovene Museum of Natural History, Prešernova 20, SI-1001 Ljubljana, Slovenia.

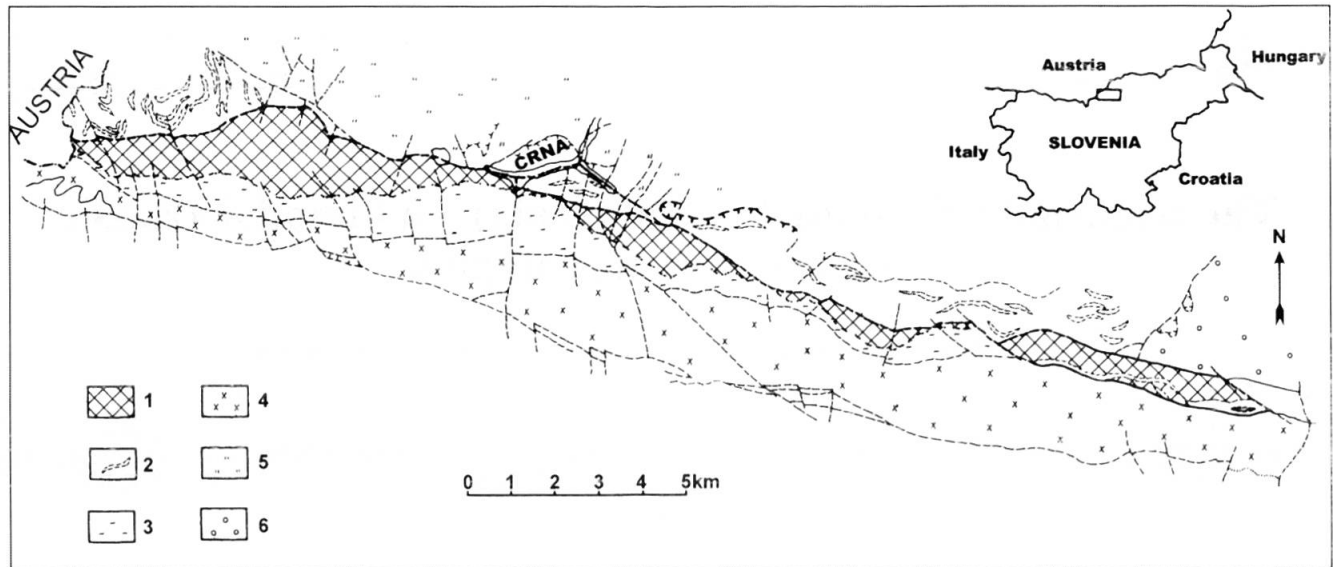


Fig. 1 Geological sketch map of the Karavanke Igneous zone and the investigated area (simplified after MIOČ and ŽNIDARČIČ, 1978). 1 = granitic belt, 2 = Paleozoic green schist with diabase lenses, 3 = fine grained gneiss, 4 = tonalite, 5 = Triassic dolomite, 6 = Miocene conglomerate.

In this work, new field, petrographic and geochemical data on rocks of the Karavanke Granitic Belt (KGB) are presented and a possible model for the genesis and evolution of this magmatic suite is proposed.

## 2. Geological setting and previous work

The central Karavanke magmatic zone consists of two parallel elongated massifs, the Northern Karavanke Granitic Belt (hereafter Granitic Belt), which is the object of the present paper, and the Southern Tonalitic Belt, related to a distinct magmatic event (FANINGER, 1976). The massifs are separated by a thin belt of metamorphic rocks (Fig. 1). The Karavanke magmatic zone lies along the Periadriatic lineament, and outcrops mainly in the northeastern part of Slovenia and partly in the Austrian area, where it is represented by the "Eisenkappel (Karawanken) Granite" and "Karawanken Tonalite Gneiss". It extends for about 35 km from the Slovene–Austrian border on the west to the Tertiary sediments of the Pannonic basin near Plešivica to the east.

The Granitic Belt is bordered by Paleozoic phyllitoid shales with diabase dikes and Triassic dolomite to the north and by a metamorphic complex to the south (MIOČ and ŽNIDARČIČ, 1978; MIOČ, 1983). Metamorphic xenoliths are common near the contacts with the country rocks. Granite intrusion caused contact metamorphism in the surrounding pelitic and quartzo-feldspathic rocks on the northern and the southern side of the

massif (EXNER, 1971; HINTERLECHNER-RAVNIK, 1978). Both contacts have later been tectonized. The contact to Triassic dolomite is tectonic.

The succession from mafic to felsic rocks of the Granitic Belt has been interpreted as the result of the evolution of the same parental magma during crystallization (EXNER, 1971, 1976; FANINGER, 1974). The porphyry syenite with rapakivi texture which appears as dikes separating diorite and granite, is considered to be a rock of mixed origin produced in the reaction zones (EXNER, 1971). Magmatic breccias with sharp-cornered fragments of ultramafic rocks inside porphyry syenite suggest that mafic rocks are older than granite, which is consistent with the differentiation series. Ultramafic fragments from magmatic breccias consist of predominant olivine (60%), partly amphibolized clinopyroxene, brown amphibole and phlogopite (all three minerals 30%), with smaller amounts of calcium feldspar (5%), magnetite, ilmenite and pyrite (5%), representing mantle rocks, crystallizing in lower crust or upper mantle (HINTERLECHNER-RAVNIK, 1988/89).

The stratigraphic age of the Granitic Belt was long a matter of debate. ISAILOVIĆ and MILIČEVIĆ (1964) found blocks of metamorphic rocks, impregnated by granite inside the tonalite massif, which suggests that the Granitic Belt is older than the Tonalitic Belt.

ŠTRUCL (1970) and FANINGER (1974) date the Granite Belt as Variscan on the stratigraphic basis that the granite intrusion caused contact metamorphism on Paleozoic phyllitoid shales. The Tonalite Belt is of Alpine age. Radiometric data

show that the Granite Belt is of Triassic age. According to LIPPOLT and PIDGEON (1974), the rocks of the Granitic Belt yielded ages of  $227 \pm 7$  Ma measured on biotite (K/Ar),  $244 \pm 8$  Ma on hornblende (K/Ar) and  $230 \pm 5$  Ma on titanite (U/Pb). SCHARBERT (1975) obtained approximately the same ages of  $224 \pm 9$  Ma and  $216 \pm 9$  Ma, dating the biotites of "granodiorite porphyry" with the Rb/Sr method. It is worth noting that according to her description, the analyzed "granodiorite porphyry" fits the petrographic character of the rocks that we would here classify as "porphyry syenite". An initial  $^{87}\text{Sr}/^{86}\text{Sr}$  isotopic value of 0.71437 was obtained on a porphyry syenite (corrected for 220 Ma) (DOLENEC, 1994). The value suggests a crustal origin for the felsic magma.

The alkaline Permo-Triassic igneous activity with ages around 270–200 Ma of the Briançonnais and Aceglia zone in the French and Italian Western Alps, and the Monzoni-Predazzo plutonic-volcanic complex, Italy (FERRARA and INNOCENTI, 1974; BONIN et al., 1987 and references therein), corresponds to the period immediately preceding the breakup and fragmentation of the Pangean continental block. BONIN et al. (1987) propose to name this collection of alkaline massifs of Permo-Triassic age, the Western Mediterranean Province.

### 3. Field relationships, petrography and mineral chemistry

The Granitic Belt is mainly composed of syenogranite and syenite with contemporaneous mafic and intermediate rocks which constitute about 30% of the whole massif. They range from decimetric, rounded enclaves, to large, decametric bodies. The shape of the large mafic bodies is not clearly recognizable due to the presence of soil and vegetation. Small mafic enclaves are medium to fine grained, with sharp contact to the syenogranite. In the vicinity of the enclaves, K-feldspar megacrysts of the host syenogranite are mantled by plagioclase. Large bodies of mafic rocks are occasionally cut by veins of porphyry syenite with rapakivi texture. In some of the intermediate rocks quartz ocelli are observed. Intrusive breccias with obvious penetration of K-feldspar megacrysts from felsic into mafic magma are present as well. Features like quartz ocelli, plagioclase mantled K-feldspar and intrusive breccia indicate that some interaction between mafic and felsic magmas has occurred.

Sampling has been carried out with the aim of collecting the various lithologies which make up the Karavanke Granitic Belt. Rocks have been

classified on chemical basis, following the BELLIENI et al. (1995) proposal. Further distinctions were based on field relationships and petrographic texture.

According to BELLIENI et al. (1995) proposal (Fig. 2) mafic rocks range from gabbro (or diorite) to monzogabbro (or monzodiorite). Intermediate rocks are represented by monzonite, whilst felsic rocks range from syenite ( $61\% < \text{SiO}_2 < 69\%$ ) to syenogranite ( $\text{SiO}_2 > 69\%$ ). In the DE LA ROCHE et al. (1980) classification diagram (Fig. 3), mafic and intermediate rocks range from: olivine gabbro, syeno gabbro, syeno diorite to monzonite, whereas the composition of felsic rocks falls along the line which separates quartz monzonites from syenite and quartz syenite as well as granite from alkali granite. The analyzed rocks belong to an alkaline series (Fig. 2). The higher abundance of  $\text{K}_2\text{O}$  than that of  $\text{Na}_2\text{O}$  (Tab. 1) indicates that, according to ZANNETIN (1986), these rocks belong to a potassic series.

It is worth noting that some authors (EXNER, 1971, 1976; FANINGER 1974, 1976; LIPPOLT and PIDGEON, 1974; SCHARBERT, 1975; MIOČ, 1983) assigned rocks of the Karavanke Granitic Belt as "gabbro, diorite, granodiorite, granite" and thus obscured the true alkaline nature of those rocks.

#### 3.1. MAFIC AND INTERMEDIATE BODIES

**Gabbro** is a fine to medium grained rock containing normal to alkaline amphiboles (Mg-hornblende and edenite after LEAKE et al. (1997)), plagioclase ( $\text{An}_{45-70}$ ) (Tab. 2) orthopyroxene ( $\text{Fs}_{22-31}$ ), and olivine ( $\text{Fo}_{73-79}$ ). Sometimes hornblende replaces pyroxene, or forms wormlike overgrowths with pale green pyroxene. In some samples, there are two generations of hornblende. The first generation is brown (edenitic composition), euhedral, while the second generation forms green (Mg-hornblende), fine grained, polycrystalline aggregates. Anhedral plagioclase grains show deformed twin lamellae. The accessory minerals are apatite in long needles, titanite, zircon, opaque minerals, and secondary epidote.

**Monzogabbro and Monzodiorite** are fine to coarse grained rocks, containing normal to alkaline amphiboles (Mg-hornblende and edenite), plagioclase, biotite and clinopyroxene of diopsidic composition ( $\text{Wo}_{48}\text{En}_{35}\text{Fs}_{17}$ ). Two generations of hornblende were recognized. The older one is brown (edenite), whilst the younger is green (Mg-hornblende). In monzodiorite, green hornblende sometimes contains a brown core. Hornblende is partly transformed to actinolite and altered to chlorite. Plagioclases are euhedral, elongated,

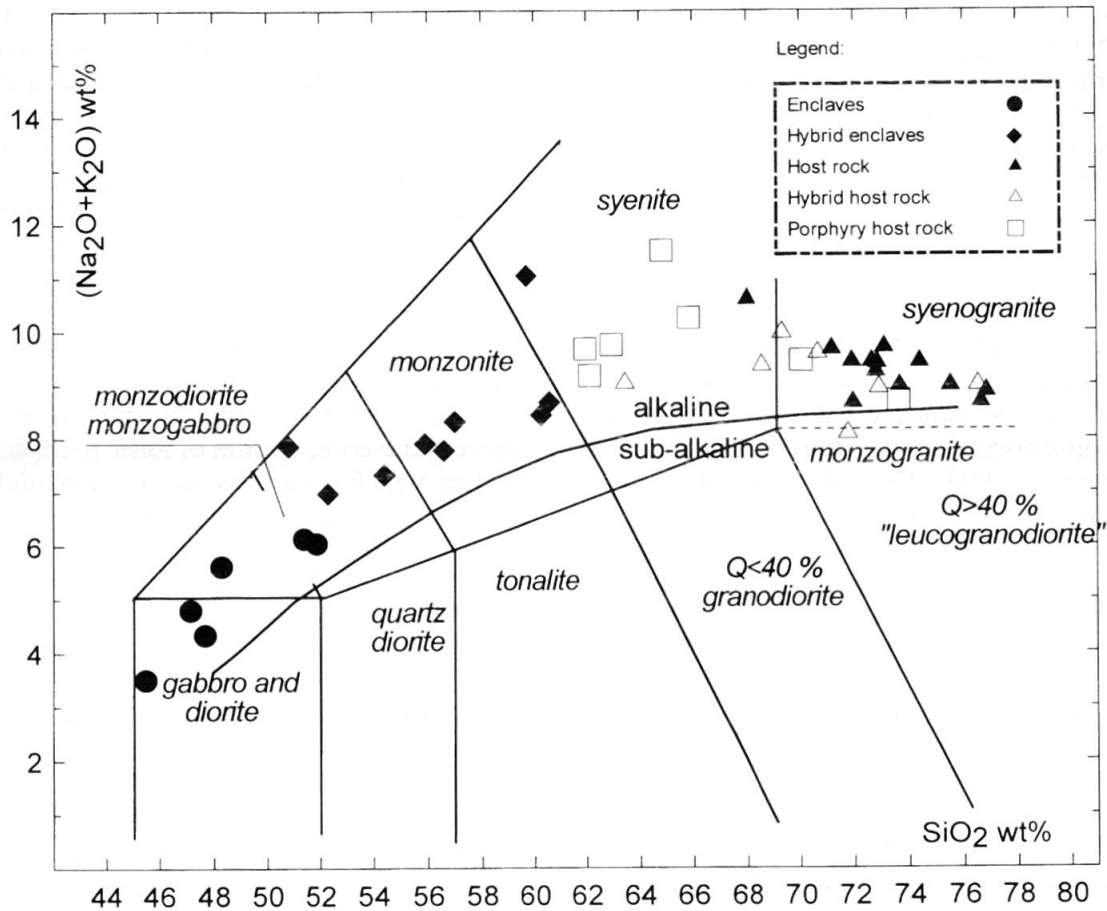


Fig. 2 Classification of KGB rock types (BELLINI et al., 1995). Alkaline-subalkaline border from MIYASHIRO (1978). Values recalculated to  $\text{Sum}_{\text{Ox}} = 100\%$ .

normally zoned ( $\text{An}_{47-28}$ ), with core altered to sericite. K-feldspar is present only in one sample of monzodiorite, in wormlike overgrowths with plagioclase. Anhedra titanite prevails among accessory minerals, and apatite, opaque minerals, secondary epidote and carbonate occur as well.

**Monzonite** is a fine grained rock, consisting of plagioclase ( $\text{An}_{30}$ ), K-feldspar, quartz of two generations, Mg-hornblende and biotite. In some samples, biotite replaces hornblende. Quartz of the first generation forms rounded grains, surrounded by hornblende and biotite, sometimes together with clinopyroxene or plagioclase. Such structure has been described in literature as quartz ocelli (BLUNDY and SPARKS, 1992). The second generation of quartz is fine grained and corrodes phenocrysts of the first generation and fills the veins and fissures in plagioclase. Monzonite contains about 1–2% of accessory apatite and zircon, secondary epidote, carbonate and opaque minerals also occur. Hornblende and biotite are often altered to chlorite.

### 3.2. HOST ROCKS

**Syenogranite** is a fine to coarse grained rock. It contains plagioclase ( $\text{An} < 3\%$ ), K-feldspar and quartz of two generations, biotite, and hornblende. Plagioclase of the first generation forms euhedral crystals, with inclusions of very small, optically undetermined minerals, indicating disturbances in their growth. They also appear as inclusions in K-feldspars and are mostly altered to sericite. The second generation is less altered, and often grows on crystals of the first generation with the same optical orientation and composition. The first generation of K-feldspar is represented by euhedral (up to 30 mm in coarse grained syenogranite) crystals of perthite or microcline-perthite, containing inclusions of plagioclase, quartz and biotite. The second generation is represented by fine grained microcline. At the contact between K-feldspar and plagioclase, microcline structure is observed. Quartz of the first generation forms rounded grains and small inclusions in K-feldspars. The second generation is fine grained, and fills intergranular space and



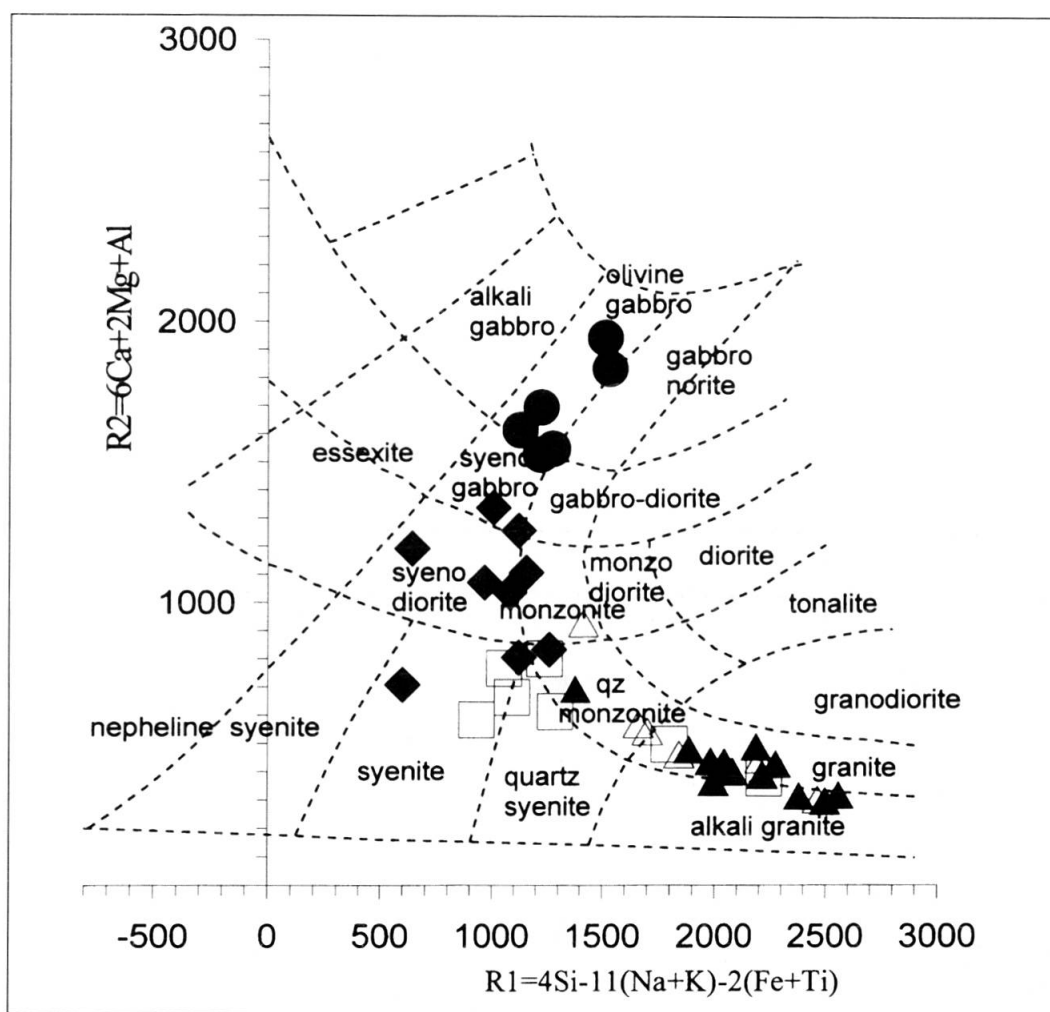


Fig. 3 Classification of KGB rock types (DE LA ROCHE et al., 1980). Symbols as in figure 2.

fissures. Biotite (annite 80–60%) and hornblende are euhedral. Hornblende rims are usually corroded by later phases (mostly quartz). In most samples, hornblende is altered to chlorite. In all felsic rocks, accessory minerals are very rare (< 0.5%) and consist of apatite, zircon and secondary epidote, allanite and clinozoisite.

**Syenogranite and syenite containing muscovite** differ from syenogranite because of muscovite growing in plagioclase cleavage cracks. Also plagioclase is more calcic ( $An_{16}$ ). The space between grains of the first generation minerals is filled by wormlike overgrowth of plagioclase, K-feldspar and quartz of the second generation.

**Porphyry syenite** has fine grained matrix of anhedral plagioclase, hornblende, biotite, K-feldspar and quartz. Phenocrysts consist of biotite (annite 60–50%), plagioclase ( $An_{15-20}$ ), quartz and euhedral perthitic K-feldspar ( $Or_{90}$ ), usually rimmed by wormlike overgrown plagioclase ( $An_{20}$ ) and quartz (Tab. 3). Euhedral K-feldspar mantled by plagioclase (oligoclase) represents rapakivi texture *sensu stricto* (RÄMÖ and HAAPALA, 1995). The cellular growth of plagioclase and in-

filling of voids with quartz may be a consequence of magma mixing (HIBBARD, 1981). Phenocrysts of ferrous hornblende occur as well. Accessory minerals like needles of apatite, zircon, secondary epidote, allanite and clinozoisite, and opaque minerals are very abundant (approx. 3–4%). In porphyry syenites with less than 64% of  $SiO_2$  content, clinopyroxene is present in the matrix.

#### 4. Geochemistry

For almost all major and some trace elements, rocks of the Karavanke Granitic Belt (Tab. 1) define a continuous trend with increasing differentiation index (D.I.) (THORNTON and TUTTLE, 1960).

Variation diagrams (Fig. 5) of major elements vs. D.I. show that the rocks of the Karavanke Granitic Belt define smooth negative trends for  $MgO$ ,  $CaO$ ,  $MnO$ ,  $TiO_2$  and  $FeO_t$  and positive for  $SiO_2$ ,  $Na_2O$  and  $P_2O_5$  tend to increase up to the intermediate D.I. values and decrease for higher D.I.  $Al_2O_3$  remains constant, for D.I. < 80 and decreases at higher D.I. values. Note that, mainly for felsic

and intermediate rocks with D.I. > 60, Na<sub>2</sub>O, K<sub>2</sub>O and P<sub>2</sub>O<sub>5</sub> show a wide range of values for rocks with similar degrees of differentiation.

Such dispersion of values is particularly evident in the trace elements vs. D.I. diagrams, where the contents of many trace elements (Y, Zr, Nb, Nd, Ce, La) of felsic and mafic rocks are similar (Fig. 6). Nevertheless, Zr, Nd, Ce, La, Ba show an overall positive correlation for mafic rocks, and a negative correlation for felsic rocks, whereas the rocks of intermediate composition show a wide range of values for these elements.

All rocks show a strong fractionation of LREE ((La/Sm)<sub>N</sub>=2.38–8.48), which increases from mafic to felsic rock types (Fig. 7). HREE are

slightly fractionated ((Gd/Yb)<sub>N</sub>= 0.75–2.81) in the mafic rocks and almost not fractionated ((Gd/Yb)<sub>N</sub>= 0.69–1.34) in the felsic rocks. All rocks except gabbro show a moderate to strong negative Eu anomaly (Eu/Eu\* = 0.24–0.99), which tends to increase from mafic to felsic samples. Only a few samples of porphyry syenite and syenogranite show a positive Eu anomaly (Eu/Eu\* = 1.10–2.03).

## 5. Discussion

Several features, observed in the Karavanke Granite Belt indicate that some rock types were formed by the interaction of felsic and mafic mag-

Tab. 1 Major (wt%), trace element (ppm) and REE (ppm) data for KGB rock types. Major, trace and RE elements were determined at Actalab, Canada. ICP was used for major elements whilst INAA and ICP-MS for trace and RE elements.

SAMPLE	Host rock (syenogranite and syenite)												
	G5d	G8c	G8a	G8b	G5e	G16	G18a	G18gr	G18b	G15a	G1i	G1f	G24b
SiO <sub>2</sub>	75.16	75.16	73.84	73.63	72.85	72.65	72.33	71.28	71.24	70.71	70.64	69.19	65.77
TiO <sub>2</sub>	0.13	0.09	0.13	0.18	0.21	0.26	0.25	0.35	0.34	0.27	0.31	0.31	0.36
Al <sub>2</sub> O <sub>3</sub>	12.51	12.60	13.75	13.30	13.83	14.30	14.10	14.13	14.36	13.43	13.97	14.38	14.17
FeOt	1.15	0.91	1.16	1.31	1.61	1.87	1.76	2.50	2.10	2.06	1.86	2.05	2.17
MnO	0.03	0.02	0.03	0.02	0.05	0.06	0.05	0.06	0.06	0.06	0.05	0.06	0.05
MgO	0.22	0.18	0.12	0.02	0.29	0.36	0.35	0.54	0.48	0.48	0.49	0.42	0.67
CaO	0.35	0.15	0.85	0.25	1.11	0.76	0.44	1.51	1.02	1.10	0.69	1.35	3.19
Na <sub>2</sub> O	3.93	4.21	4.11	4.12	3.96	4.41	4.52	4.11	4.39	4.23	4.39	4.25	4.83
K <sub>2</sub> O	4.57	4.46	5.24	4.63	4.91	4.97	5.07	4.47	4.95	4.95	4.58	5.15	5.42
P <sub>2</sub> O <sub>5</sub>	0.04	0.03	0.03	0.07	0.08	0.10	0.10	0.14	0.14	0.11	0.13	0.12	0.17
LOI	0.51	0.50	0.42	0.81	0.47	0.78	0.77	0.52	0.69	1.14	0.86	0.57	2.78
sum	98.72	98.33	99.72	98.21	99.52	100.74	99.93	99.86	98.55	98.73	97.09	96.41	99.73
Ba	130.60	179.90	251.70	138.10	264.10	263.60	235.40	356.10	260.20	248.20	271.90	257.90	295.20
Cs	4.30	4.80	16.20	6.60	12.30	10.20	5.30	14.30	6.10	5.20	4.00	5.90	4.10
Ga	17.00	17.00	20.00	20.00	17.00	17.00	17.00	20.00	19.00	18.00	17.00	20.00	17.00
Hf	4.20	3.40	4.60	5.50	3.90	4.90	5.20	5.90	5.50	5.90	4.90	5.50	5.80
Nb	46.00	31.10	32.40	37.30	27.80	26.60	30.40	35.00	39.50	31.20	30.50	32.20	32.10
Ni	54.00	43.00	38.00	44.00	32.00	19.00	23.00	58.00	75.00	33.00	15.00	43.00	46.00
Pb	5.00	5.00	18.00	11.00	12.00	6.00	7.00	17.00	9.00	7.00	5.00	15.00	41.00
Rb	244.20	245.90	286.20	257.20	236.60	227.10	215.90	223.70	208.80	214.50	193.30	194.30	165.30
Sr	76.20	57.50	117.00	85.50	167.90	198.80	197.40	191.10	218.50	157.60	181.10	208.20	236.10
Ta	4.37	3.79	3.84	4.98	3.57	2.24	3.64	3.78	4.03	3.13	3.30	3.44	2.92
Th	37.84	27.89	30.44	46.13	24.99	31.23	27.10	26.65	33.30	30.00	29.43	27.60	24.03
Tl	0.80	1.30	1.90	2.10	1.60	1.30	1.10	2.70	0.70	0.70	0.40	0.80	2.10
V	18.00	17.00	18.00	33.00	20.00	19.00	28.00	20.00	28.00	28.00	32.00	27.00	25.00
W	5.70	6.50	6.60	6.50	10.20	2.10	3.80	5.00	3.00	4.90	3.60	4.50	2.80
Y	27.00	15.00	13.00	20.00	17.00	19.00	13.00	18.00	22.00	21.00	16.00	20.00	14.00
Zr	110.30	82.50	112.00	146.80	114.30	145.80	158.40	192.90	173.70	173.70	161.00	169.40	211.70
La	21.20	23.00	12.10	20.40	20.20	33.10	31.50	24.30	45.90	32.50	33.20	25.40	35.30
Ce	44.70	81.20	35.70	63.80	40.60	63.80	64.80	51.00	86.70	65.20	67.70	50.00	64.70
Pr	3.98	4.04	2.24	3.73	3.78	5.76	4.46	4.19	6.71	5.67	5.65	4.76	4.94
Nd	16.60	14.60	8.40	13.40	14.90	23.40	17.00	18.30	27.70	23.30	21.10	19.70	19.80
Sm	3.60	2.50	1.90	2.60	3.00	4.20	3.00	3.30	4.20	4.00	3.60	3.90	3.40
Eu	0.29	0.27	0.39	0.26	0.60	0.69	0.63	0.78	0.84	0.62	0.68	0.67	0.82
Gd	3.70	2.80	1.70	3.00	3.00	3.60	2.80	3.20	4.50	3.90	2.90	3.50	3.40
Tb	0.70	0.40	0.30	0.50	0.50	0.60	0.40	0.50	0.70	0.60	0.50	0.60	0.50
Dy	4.80	2.50	2.20	3.40	3.00	3.60	2.60	3.20	3.80	3.80	3.00	3.80	2.80
Ho	1.00	0.60	0.50	0.70	0.60	0.60	0.50	0.60	0.80	0.70	0.60	0.70	0.50
Er	3.50	1.90	1.60	2.40	1.80	2.00	1.60	2.00	2.50	2.30	1.90	2.20	1.50
Tm	0.55	0.30	0.30	0.40	0.32	0.31	0.24	0.31	0.33	0.34	0.28	0.36	0.23
Yb	3.80	2.30	2.00	3.20	2.10	2.30	1.80	2.60	2.70	2.70	2.20	2.50	1.70
Lu	0.64	0.38	0.31	0.53	0.35	0.35	0.30	0.38	0.44	0.41	0.34	0.39	0.25

ma: like K-feldspar megacrysts, with or without rapakivi rim (porphyry syenite); quartz ocelli (monzonite); the disturbances in plagioclase zoning (syenite containing muscovite); the high content of hornblende and biotite (high  $P_{H_2O}$ ) (monzodiorite, monzogabbro); and the wide range of values for some major and most of the trace elements (rocks of intermediate composition) (HIBBARD, 1981; ZORPI, 1988; BUSSY, 1990; DIDIER and BARBARIN, 1991 and references therein; RÄMÖ and HAAPALA, 1995). Petrographic analyses show that in all porphyry rocks the matrix is more mafic and phenocrysts are more felsic, suggesting that felsic phenocrysts were introduced into mafic magma. The rapakivi texture, K-feldspar with oligoclase rim forming a wormlike overgrowth with quartz observed in porphyry rocks in-

dicates the intrusion of partly crystallized granitic magma containing K-feldspar megacrysts into a more mafic magma (HIBBARD, 1981; BUSSY, 1990).

In monzonite, quartz ocelli are surrounded by fine grained hornblende, pyroxene and biotite. According to VERNON (1991), this indicates the hybrid nature of the magmas. The instability of quartz grains introduced into mafic magma causes melting of the xenocryst rims. The melting uses latent heat of crystallization from adjacent melt. This locally increases the undercooling and nucleation rate, which causes the formation of fine grained aggregate of minerals that are saturated in the crystallizing magma. Such structures form during rapid cooling. When the cooling rate is lower, quartz precipitates from the evolved and modified melt, and forms the overgrowths with

Tab. 1 (cont.)

SAMPLE	Hybrid host rock							Porphyry syenite						
	G6a	G17	G13b	G19	G25a	G23a	G13c	P24a	P3bd	P1g	P18e	P6b	P28a	P13gp
SiO <sub>2</sub>	76.37	71.19	70.60	68.47	68.12	68.03	64.58	72.43	68.80	65.25	64.90	60.83	60.65	60.28
TiO <sub>2</sub>	0.09	0.21	0.32	0.41	0.43	0.41	0.45	0.42	0.42	0.74	0.59	0.83	0.81	1.09
Al <sub>2</sub> O <sub>3</sub>	12.95	14.40	14.75	14.53	16.17	15.26	18.27	13.42	14.72	15.41	16.30	16.80	17.57	16.81
FeOt	1.00	2.12	3.12	2.50	2.97	1.97	3.4	4.53	2.65	3.84	2.14	4.82	4.71	3.46
MnO	0.02	0.05	0.04	0.05	0.05	0.03	0.05	0.02	0.07	0.07	0.13	0.10	0.07	0.10
MgO	0.17	0.30	0.62	0.60	0.64	0.50	0.64	0.53	0.60	1.00	0.91	1.34	1.34	1.40
CaO	0.19	0.60	0.92	1.07	1.61	2.02	4.99	0.75	1.57	2.38	2.04	2.28	3.45	3.23
Na <sub>2</sub> O	4.14	3.96	4.81	4.34	4.81	4.55	4.99	4.71	4.63	4.73	4.86	5.33	4.90	5.24
K <sub>2</sub> O	4.83	4.76	3.14	4.95	4.48	5.23	4.21	3.84	4.66	5.43	6.66	4.09	4.06	4.17
P <sub>2</sub> O <sub>5</sub>	0.03	0.12	0.09	0.07	0.07	0.16	0.15	0.13	0.16	0.28	0.25	0.38	0.36	0.40
LOI	0.45	0.74	0.96	1.00	0.95	0.79	0.98	0.67	0.72	0.60	0.36	1.42	0.72	0.51
sum	99.15	95.72	99.65	98.27	100.72	99.10	100.15	99.31	99.33	100.22	98.31	98.56	95.71	94.51
Ba	164.50	174.60	196.60	328.40	362.80	415.50	329.70	365.20	335.70	349.50	264.10	390.30	529.80	431.10
Cs	5.20	4.00	2.00	3.70	4.30	2.20	4.10	2.30	4.30	6.60	22.80	5.30	3.50	3.30
Ga	19.00	18.00	20.00	20.00	19.00	18.00	22.00	16.00	20.00	24.00	25.00	24.00	23.00	23.00
Hf	3.60	6.90	6.90	6.40	3.20	4.90	8.60	5.10	5.40	6.60	11.00	10.40	10.50	6.30
Nb	31.30	18.30	21.50	34.80	15.30	18.50	19.70	20.50	32.50	38.60	65.20	55.90	32.90	48.30
Ni	56.00	32.00	51.00	31.00	27.00	34.00	37.00	37.00	50.00	41.00	34.00	46.00	34.00	35.00
Pb	5.00	26.00	19.00	17.00	12.00	6.00	16.00	12.00	18.00	14.00	16.00	17.00	9.00	15.00
Rb	260.30	127.70	92.70	171.40	136.70	117.40	104.60	90.50	163.90	163.40	381.00	150.40	106.30	103.80
Sr	60.40	104.00	203.50	247.70	371.70	529.70	279.10	276.20	287.70	321.80	237.30	462.00	507.00	446.10
Ta	4.43	1.20	1.46	3.07	1.13	1.10	1.26	1.65	2.46	3.10	5.51	4.03	2.27	2.59
Th	29.24	21.22	27.90	23.98	13.25	16.83	23.91	29.69	23.69	20.57	24.58	21.17	14.59	10.40
Tl	2.90	1.40	1.40	1.50	0.90	0.60	1.60	1.00	1.40	1.60	3.20	1.80	0.50	0.80
V	15.00	21.00	17.00	24.00	12.00	24.00	31.00	37.00	24.00	47.00	29.00	52.00	55.00	73.00
W	5.90	2.50	5.10	2.60	1.80	1.90	2.50	2.80	2.60	3.10	1.90	2.30	1.50	1.20
Y	14.00	8.00	12.00	17.00	10.00	13.00	16.00	8.00	20.00	21.00	28.00	38.00	21.00	21.00
Zr	78.70	251.50	218.70	213.10	93.00	168.70	342.50	166.40	182.30	218.00	408.40	359.80	385.90	250.10
La	15.50	54.80	40.50	26.00	18.30	26.30	64.70	29.10	43.20	34.00	43.50	32.10	47.00	35.80
Ce	51.30	100.60	86.80	52.70	36.50	50.70	116.80	51.70	84.70	68.40	93.80	75.90	88.90	75.60
Pr	3.13	7.84	6.71	4.50	3.21	4.24	9.06	4.04	7.23	6.30	7.99	7.66	7.72	6.88
Nd	11.20	29.90	26.00	20.40	14.00	19.00	34.00	15.20	28.60	27.80	34.00	37.00	32.10	31.00
Sm	2.10	4.00	4.10	3.90	2.40	3.30	4.80	2.30	4.50	5.10	5.80	7.60	5.60	5.80
Eu	0.26	0.52	0.53	0.91	1.56	1.18	1.06	0.93	1.07	1.36	0.97	1.50	1.58	1.46
Gd	2.10	3.50	3.70	3.60	2.20	3.10	4.70	2.30	4.50	4.80	5.80	6.90	5.20	5.40
Tb	0.30	0.40	0.50	0.60	0.40	0.50	0.60	0.30	0.60	0.70	0.90	1.30	0.70	0.80
Dy	2.20	1.70	2.50	3.20	2.00	2.50	2.80	1.80	3.80	4.20	5.30	7.10	3.90	4.40
Ho	0.50	0.30	0.50	0.70	0.40	0.50	0.60	0.30	0.70	0.80	1.10	1.40	0.70	0.80
Er	1.60	1.00	1.50	2.00	1.20	1.50	1.70	0.90	2.20	2.40	3.40	4.10	2.30	2.40
Tm	0.30	0.14	0.22	0.28	0.15	0.19	0.26	0.11	0.28	0.33	0.46	0.58	0.29	0.29
Yb	2.20	1.10	1.50	2.00	1.10	1.40	2.10	0.90	2.40	2.60	3.90	4.20	2.30	1.90
Lu	0.35	0.15	0.26	0.33	0.18	0.17	0.38	0.16	0.37	0.38	0.61	0.66	0.35	0.29



mafic minerals in xenocryst rims (VERNON, 1991; PLATEVOET and BONIN, 1991).

In most of the major elements vs. D.I. diagrams (Fig. 5), the rocks of the Karavanke Granitic Belt form a continuous series. The most mafic rock sample (D.I. < 25 – olivine gabbro) is enriched in MgO and depleted in CaO and Al<sub>2</sub>O<sub>3</sub> with respect to the mafic series. The deviation can be explained by small amount of olivine cumulation in the sample.

In the trace elements vs. D.I. as well as in the P<sub>2</sub>O<sub>5</sub> and TiO<sub>2</sub> vs. D.I. (Figs 5, 6) we observe strong dispersion of values for rocks of intermediate composition. On the other hand the content of most trace elements is similar for mafic and felsic rocks (Y, Zr, Nb, Nd, Ce, La, Ba), increasing in mafic series towards intermediate rocks values

and decreasing in felsic series. The behaviour of trace elements indicates the bimodal composition of the complex, with different magma source for felsic and mafic magmas. The dispersed values of trace elements in rocks of intermediate composition are due to different stages of interaction of felsic and mafic magma. The enrichment of trace elements (Y, Zr, Nb, Nd, Ce, La, Ba) in the intermediate rocks, to values higher than in mafic or felsic rocks, may be explained by the fact that high-charge-density (HCD) cations are preferably partitioned into the mafic part of the coexisting mafic and felsic magmas (EBY, 1983). The sample with D.I. of 54 is particularly enriched in Cs, Zr, Nb, Nd, Ce, La, Sr and P<sub>2</sub>O<sub>5</sub>, due to high content of accessory minerals – titanite and apatite.

Tab. 1 (cont.)

SAMPLE	Hybrid enclaves									Enclaves					
	M27a	M4a	M27c	M13Cb	M1c	M13Ba	M28f	M13Ca	M19a	M21a	M13d	M1a	M2a	M28e	M101k
SiO <sub>2</sub>	58.60	58.50	58.19	56.60	55.35	55.22	53.22	51.11	49.67	50.19	49.32	46.58	46.25	46.17	43.70
TiO <sub>2</sub>	1.07	1.07	1.06	2.40	1.64	2.11	1.63	2.51	2.64	2.06	2.21	2.30	4.12	2.62	1.79
Al <sub>2</sub> O <sub>3</sub>	16.99	17.71	16.26	14.64	16.49	17.59	17.22	16.38	16.37	17.56	16.22	16.93	16.09	15.96	10.30
FeOt	7.03	5.53	6.51	8.22	7.59	7.39	8.11	9.12	10.30	7.83	8.50	9.22	10.99	10.53	
MnO	0.11	0.13	0.13	0.16	0.17	0.13	0.16	0.15	0.23	0.15	0.15	0.14	0.15	0.17	0.18
MgO	1.35	1.30	1.70	3.36	2.55	2.37	3.20	4.07	4.41	4.17	5.58	6.77	5.72	6.06	17.80
CaO	3.56	2.63	3.69	5.36	5.90	5.56	6.83	7.31	5.84	8.83	8.12	11.47	9.92	8.67	6.28
Na <sub>2</sub> O	5.59	5.00	4.27	3.97	4.38	5.28	4.22	4.27	4.44	3.96	3.76	2.69	3.13	3.28	2.17
K <sub>2</sub> O	2.62	5.82	4.07	4.29	3.23	2.54	2.95	2.55	3.25	1.89	2.13	1.55	1.58	2.09	1.19
P <sub>2</sub> O <sub>5</sub>	0.52	0.42	0.44	0.36	0.67	0.72	0.47	0.49	0.87	0.40	0.36	0.26	0.35	0.51	0.30
LOI	1.58	1.04	0.96	0.76	0.76	1.01	1.24	0.51	0.94	1.76	1.40	1.93	1.18	2.21	0.85
sum	99.59	99.63	97.91	100.98	99.38	100.67	99.96	99.25	91.20	99.90	90.65	100.63	100.47	99.54	98.30
Ba	263.80	484.80	409.90	263.70	375.00	575.10	301.30	274.80	350.30	264.50	236.30	191.90	219.90	290.00	94.00
Cs	3.00	5.00	3.90	2.80	6.90	6.30	4.40	3.50	38.90	3.10	5.10	4.40	4.30	3.80	3.50
Ga	26.00	24.00	23.00	22.00	25.00	24.00	22.00	23.00	24.00	21.00	20.00	21.00	18.00	22.00	16.00
Hf	5.80	12.70	7.00	6.20	6.60	6.20	4.70	6.90	9.90	5.00	4.60	3.50	4.30	5.80	3.20
Nb	37.80	64.10	40.00	34.70	45.00	71.00	31.60	40.40	95.70	38.70	32.60	19.50	30.00	43.40	23.00
Ni	20.00	27.00	31.00	32.00	42.00	23.00	27.00	37.00	41.00	47.00	51.00	85.00	33.00	66.00	447.00
Pb	13.00	16.00	6.00	10.00	13.00	10.00	5.00	6.00	5.00	9.00	5.00	5.00	5.00	9.00	1.90
Rb	103.20	218.60	116.10	143.10	132.00	97.90	108.40	60.00	171.90	95.60	59.50	49.90	41.00	101.90	30.00
Sr	510.30	478.50	477.50	413.30	623.40	748.30	595.50	612.60	988.40	887.20	652.00	698.00	630.60	641.00	335.00
Ta	2.63	3.80	2.68	2.42	2.95	4.93	2.35	2.56	5.88	2.46	2.07	1.21	2.01	2.68	1.50
Th	13.41	15.56	13.40	15.24	15.58	11.85	10.75	7.44	6.73	5.06	4.80	2.66	3.80	4.77	3.70
Tl	0.90	1.90	0.70	1.60	2.00	0.70	0.60	0.50	2.10	1.20	0.40	0.30	0.10	1.20	0.09
V	46.00	41.00	57.00	222.00	109.00	141.00	210.00	228.00	165.00	203.00	228.00	276.00	343.00	271.00	205.00
W	2.90	2.00	2.90	2.40	1.90	2.40	4.50	1.70	2.10	2.00	0.60	1.00	0.60	2.70	0.90
Y	27.00	31.00	27.00	23.00	25.00	28.00	29.00	23.00	27.00	21.00	22.00	19.00	19.00	26.00	17.00
Zr	188.80	483.10	250.50	200.70	240.10	211.80	153.50	252.10	383.00	176.50	164.20	117.10	133.20	211.30	120.00
La	40.60	54.30	46.20	27.80	43.10	53.30	39.50	33.40	61.80	28.60	26.80	20.00	20.80	32.70	16.30
Ce	89.00	110.70	97.60	63.70	92.40	113.50	88.00	72.90	128.20	61.30	59.80	36.30	48.40	70.80	35.60
Pr	8.20	9.88	8.53	6.35	8.66	10.30	8.48	6.92	11.64	6.07	5.90	4.12	5.01	7.05	4.20
Nd	38.60	43.00	37.20	28.90	40.50	44.10	37.20	32.80	53.60	28.30	29.00	22.10	25.60	33.70	18.80
Sm	6.90	7.30	7.00	6.10	7.00	7.50	7.00	6.10	8.80	5.70	5.50	4.90	5.50	6.70	4.70
Eu	1.77	1.60	2.08	1.71	2.02	2.03	2.13	1.95	2.93	1.85	2.07	1.60	1.79	2.23	1.32
Gd	6.80	6.70	6.60	5.90	6.30	7.40	7.20	5.90	8.00	5.30	5.60	4.50	5.30	6.30	4.30
Tb	1.10	1.10	1.00	0.90	1.00	1.10	1.00	1.00	1.10	0.80	0.90	0.70	0.80	1.00	0.50
Dy	5.50	6.00	5.30	4.80	5.30	5.80	5.80	5.10	6.10	4.50	4.90	4.20	4.50	5.40	3.40
Ho	1.10	1.10	1.00	0.90	1.10	1.10	1.10	1.00	1.00	0.80	0.90	0.80	0.80	1.00	0.50
Er	3.00	3.40	3.10	2.60	2.80	3.10	3.20	2.60	3.10	2.30	2.60	2.00	2.20	2.80	1.70
Tm	0.37	0.50	0.38	0.31	0.36	0.42	0.41	0.30	0.35	0.26	0.27	0.22	0.24	0.33	0.10
Yb	2.70	3.70	2.60	2.40	2.40	2.90	2.80	2.40	2.30	2.20	2.00	1.50	1.80	2.30	1.20
Lu	0.34	0.54	0.45	0.32	0.40	0.40	0.41	0.33	0.40	0.34	0.29	0.26	0.23	0.32	0.06

Tab. 2 Representative microprobe analysis of feldspars from KGB rocks. c-core, r-rim. Mineral composition data were obtained using CAMECA Camebax 799 microprobe at CNR-Centro Studi per la Geodinamica Alpina -Padova. A PAP program (POUCHOU, 1984) was used to convert X-ray counts into weight percentages of the corresponding oxides. Structural formulae were calculated on 8 oxygen basis.

SAMPLE	syenogranite		porphyry syenite		mafic enclaves									
	G8c1	G8c2	P1g r	P1g c	M4b c	M4b r	M4b r	M19a c	M19a c	M19a c	M19a r	M19a r	M101k	M101k
SiO <sub>2</sub>	69.42	68.02	65.01	64.66	59.49	65.31	59.23	61.4	58.13	57.38	62.28	60.93	51.14	51.06
TiO <sub>2</sub>	0.01	0.01	0.04	0.00	0.00	0.05	0.00	0.00	0.00	0.00	0.00	0.00	0.00	0.00
Al <sub>2</sub> O <sub>3</sub>	20.02	20.18	22.53	22.38	25.02	23.46	26.14	24.96	26.53	26.46	24.12	25.37	31.7	30.95
Fe <sub>2</sub> O <sub>3</sub>	0.00	0.00	0.00	0.00	0.00	0.00	0.00	0.00	0.00	0.00	0.00	0.00	0.00	0.00
FeO	0.07	0.07	0.17	0.10	0.15	0.11	0.06	0.12	0.35	0.31	0.27	0.08	0.00	0.00
CaO	0.08	0.16	3.69	3.69	6.92	0.77	8.18	6.34	8.87	8.68	5.91	5.27	14.62	14.01
Na <sub>2</sub> O	11.14	10.73	9.11	9.03	7.21	8.46	6.82	6.02	6.31	6.03	7.86	7.37	3.18	3.67
K <sub>2</sub> O	0.07	0.13	0.30	0.30	0.27	2.75	0.15	0.12	0.31	0.23	0.42	0.66	0.01	0.00
Ox <sub>Tot</sub>	100.9	99.33	100.9	100.2	99.19	101	100.6	99.01	100.6	99.09	100.9	99.69	100.83	100.02
Si	2.997	2.982	2.841	2.844	2.673	2.852	2.63	2.732	2.593	2.592	2.742	2.708	2.308	2.324
Ti	0.000	0.000	0.001	0.000	0.000	0.002	0.000	0.000	0.000	0.000	0.000	0.000	0.000	0.000
Al	1.019	1.043	1.160	1.160	1.325	1.208	1.368	1.309	1.395	1.409	1.251	1.329	1.686	1.660
Fe <sup>3+</sup>	0.000	0.000	0.000	0.000	0.000	0.000	0.000	0.000	0.000	0.000	0.000	0.000	0.000	0.000
Fe <sup>2+</sup>	0.003	0.003	0.006	0.004	0.006	0.004	0.002	0.004	0.013	0.012	0.010	0.003	0.000	0.000
Ca	0.004	0.008	0.173	0.174	0.333	0.036	0.389	0.302	0.424	0.42	0.279	0.251	0.707	0.683
Na	0.932	0.912	0.772	0.77	0.628	0.716	0.587	0.519	0.545	0.528	0.671	0.635	0.278	0.324
K	0.004	0.007	0.017	0.017	0.016	0.153	0.009	0.007	0.018	0.013	0.024	0.037	0.001	0.000
Cat <sub>tot</sub>	4.961	4.956	4.972	4.969	4.985	4.977	4.984	4.877	4.991	4.974	4.979	4.964	4.985	5.003
An	0.40	0.83	17.82	17.99	33.82	3.91	39.43	36.21	42.27	43.17	28.31	27.07	71.54	67.73
Ab	98.81	98.03	79.65	79.74	63.72	78.24	59.45	62.19	54.41	54.28	68.14	68.57	28.12	31.97
Or	0.43	0.80	1.72	1.77	1.60	16.71	0.89	0.84	1.75	1.33	2.40	4.01	0.06	0.01

Tab. 3 Microprobe analysis of plagioclase mantled K-feldspar in porphyry syenite P1g. Measuring points 1-6 are located as shown in figure 4.

Measuring point No.						
	1	2	3	4	5	6
SiO <sub>2</sub>	64.42	64.16	64.46	64.39	65.44	66.00
TiO <sub>2</sub>	0.00	0.00	0.03	0.03	0.00	0.00
Al <sub>2</sub> O <sub>3</sub>	22.77	22.40	18.20	18.24	21.82	21.17
FeO	0.20	0.14	0.10	0.05	0.06	0.00
Fe <sub>2</sub> O <sub>3</sub>	0.00	0.00	0.00	0.00	0.00	0.00
CaO	4.21	3.92	0.04	0.06	2.89	2.25
Na <sub>2</sub> O	9.02	9.15	0.44	0.45	9.70	10.41
K <sub>2</sub> O	0.35	0.30	15.59	15.59	0.19	0.06
Ox <sub>Tot</sub>	101.1	100.2	98.93	98.83	100.1	99.93
Si	2.819	2.829	3.003	3.002	2.874	2.901
Ti	0.000	0.000	0.001	0.001	0.000	0.000
Al	1.174	1.164	0.999	1.002	1.129	1.097
Fe <sup>2+</sup>	0.007	0.005	0.004	0.002	0.002	0.000
Fe <sup>3+</sup>	0.000	0.000	0.000	0.000	0.000	0.000
Ca	0.197	0.185	0.002	0.003	0.000	0.002
Na	0.765	0.782	0.04	0.041	0.826	0.887
K	0.019	0.017	0.927	0.927	0.011	0.003
Cat <sub>tot</sub>	4.986	4.987	4.979	4.98	4.979	4.995
An	19.86	18.70	0.19	0.32	13.95	10.62
Ab	77.05	78.92	4.12	4.21	84.65	88.96
Or	1.96	1.70	95.04	95.17	1.09	0.32

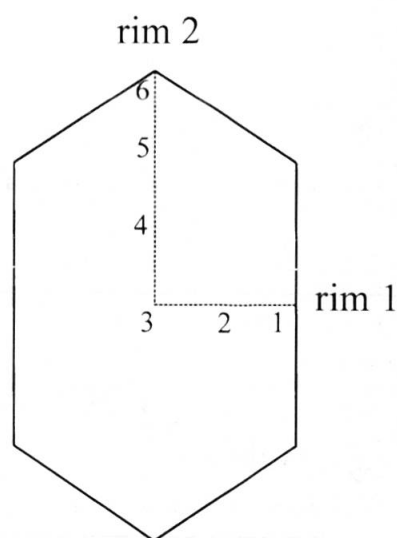


Fig. 4 Distribution of measuring points of microprobe analysis on plagioclase mantled K-feldspars in porphyry syenite.

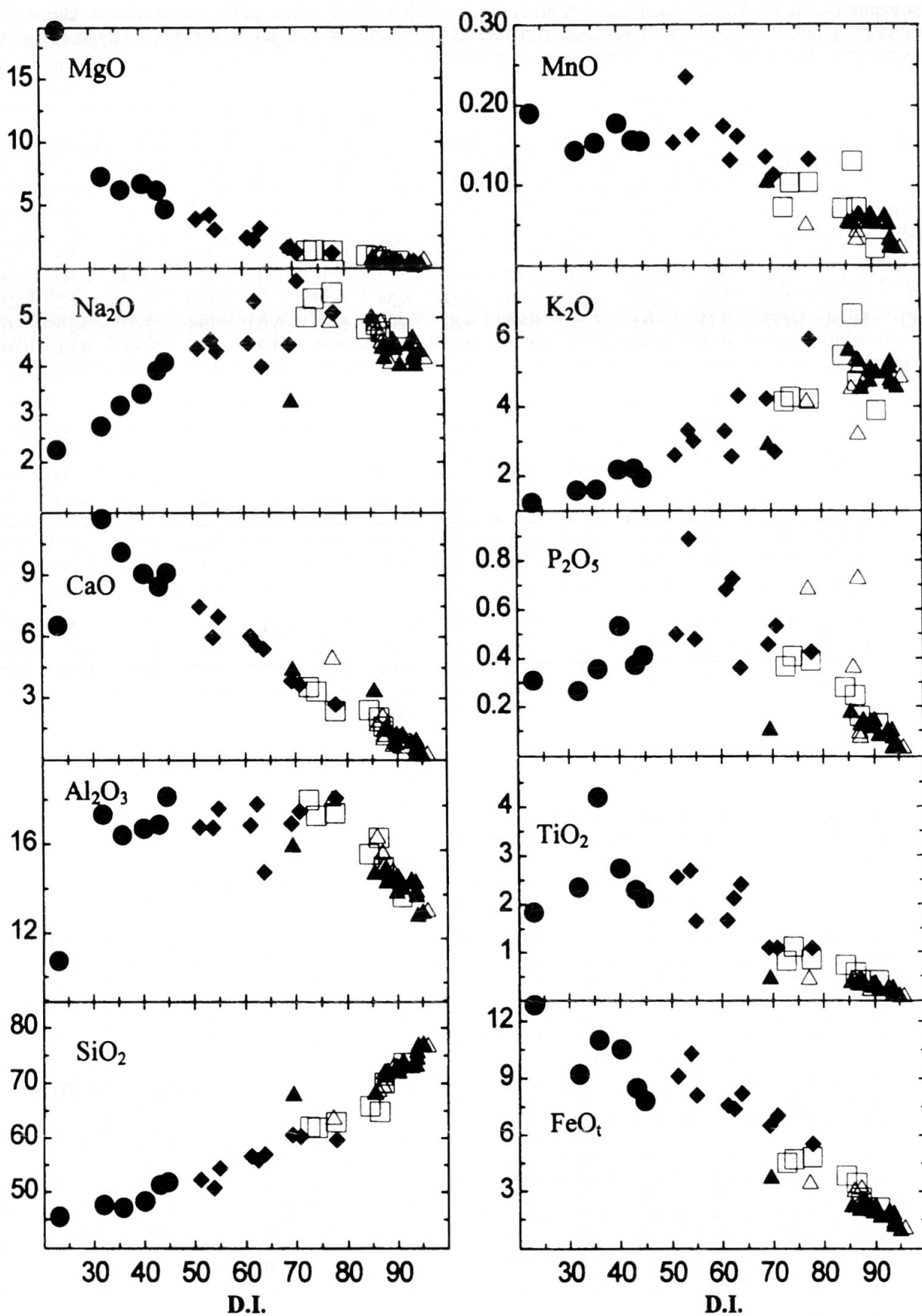


Fig. 5 Major elements (wt%) vs. D.I. for rocks of the KGB. FeO<sub>t</sub> as total FeO. Values recalculated to Sum<sub>Ox</sub> = 100%. Symbols as in figure 2.

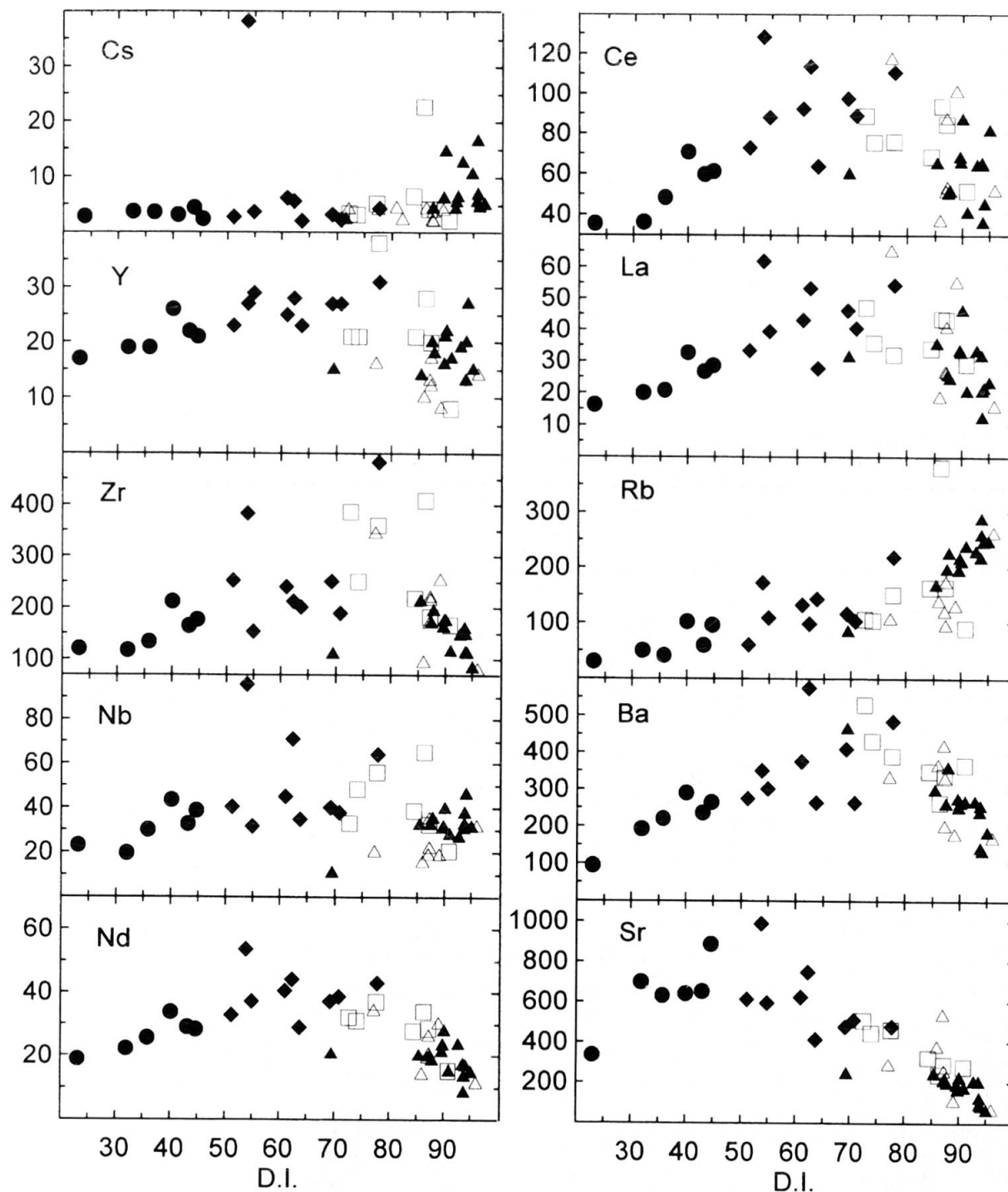


Fig. 6 Trace elements (ppm) vs. D.I. for rocks of the KGB. Symbols as in figure 2.

REE patterns (Fig. 7) also support the hypothesis of hybrid rock formation. The mafic and intermediate rocks with obvious signs of hybridization are enriched in REE with respect to the mafic rocks with no signs of hybridization. The enrichment is higher for HREE and lower for LREE. Mafic to intermediate hybrid rocks also show slight negative Eu anomaly ( $\text{Eu}/\text{Eu}^* = 0.68-0.97$ ), which is absent in non-hybrid mafic rocks ( $\text{Eu}/\text{Eu}^* = 0.99-1.12$ ). On the other hand felsic

hybrid rocks are depleted in LREE with respect to non-hybrid felsic rocks and exhibit small negative to positive Eu anomaly ( $\text{Eu}/\text{Eu}^* = 0.67-2.03$ ) except for three samples, with negative Eu anomaly similar to non-hybrid felsic rocks. In porphyry rocks, REE values are similar to non-hybrid felsic rocks values, but less fractionated in HREE part and exhibit smaller negative to slight positive Eu anomaly ( $\text{Eu}/\text{Eu}^* = 0.62-1.22$ ) with respect to non-hybrid felsic rocks.



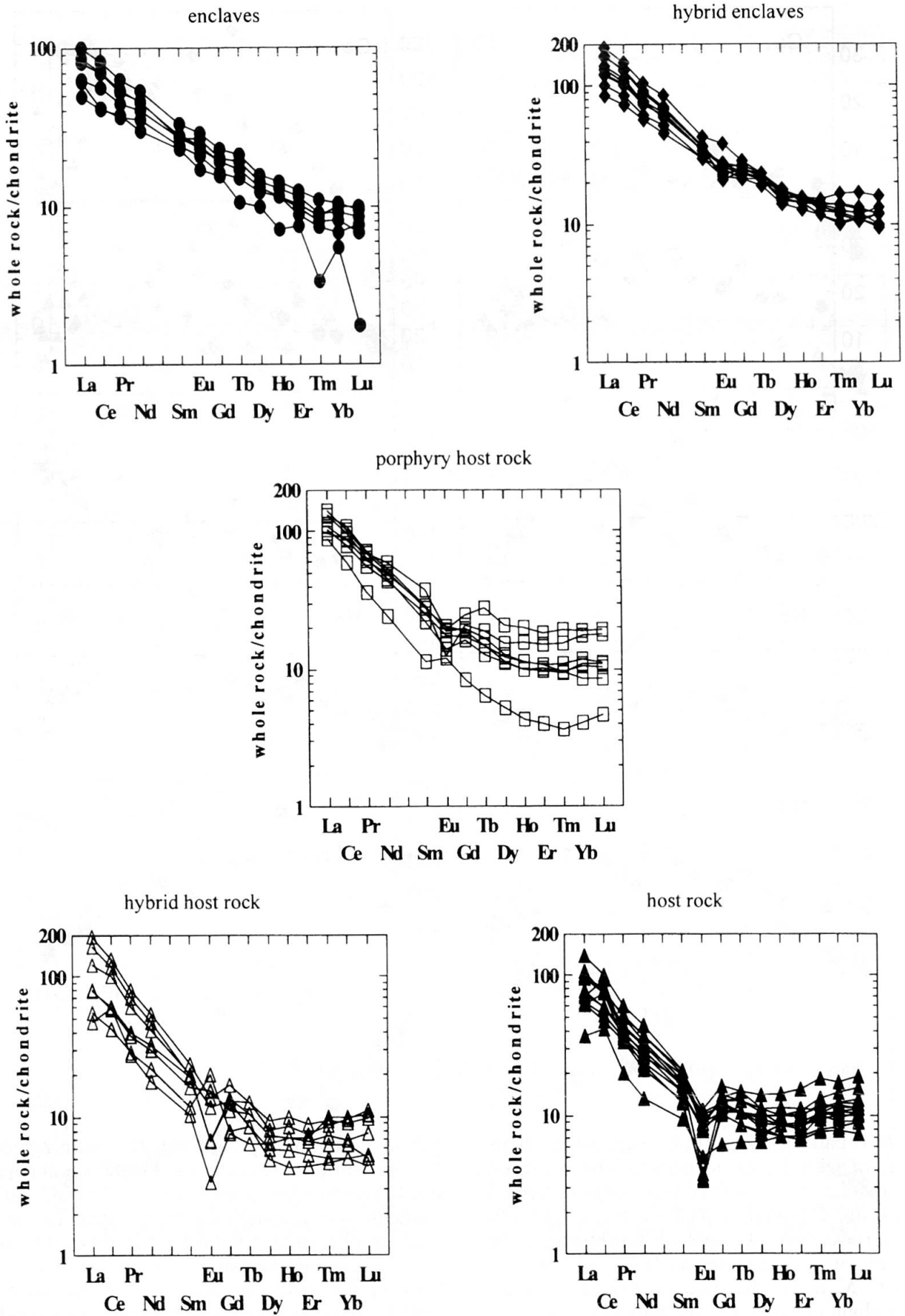


Fig. 7 Chondrite-normalized REE patterns for rocks of the KGB. Chondrite values from NAKAMURA (1974). Symbols as in figure 2.

## 5.1. MAFIC ROCKS

On the basis of field, petrographic and geochemical evidence we can divide the mafic rocks of the Karavanke Granitic Belt into two groups:

- (1) the rocks without signs of hybridization (gabbro),
- (2) hybrid rocks (monzogabbro, monzonite, monzodiorite).

Mineral and geochemical characteristics of the mafic rocks suggest the origin of the mafic magma in partial melting of the upper mantle. Relatively flat mafic rocks REE MORB normalized pattern from Nb to Yb (Fig. 8) indicate a common mantle source and the LIL enrichment is a relatively common feature in within-plate basalt provinces (BONIN 1990, 1997).

With respect to trace elements only some of the mafic rocks could be linked by the process of crystal fractionation. For La enrichment in mafic magma from 20.8 (M2a – the most mafic non-cumulative sample) up to 61.8 (M19a – the highest La value), about 72% of crystallization is needed, which would produce a residual liquid

with  $\text{SiO}_2$  content higher than 49.67%. Calculation was made for gabbro normative modal composition and mineral/melt partition coefficients from literature (ROLLINSON, 1993). The La enrichment might be reasonably explained by the process of crystal fractionation for the La value up to 28.6 (M21a – D.I. = 45). All other mafic and intermediate rocks probably underwent hybridization.

## 5.2. FELSIC ROCKS

Felsic rocks of Karavanke Granite Belt – syenogranite – are meta- to peraluminous ( $A/CNK = 0.85\text{--}1.2$ ), transsolvus (mesoperthitic alkali feldspar + K-feldspar + albite) (BONIN, 1991, SHAND in CLARKE, 1992).

In the PEARCE et al. (1984) Rb/Y+Nb discrimination diagram for the tectonic interpretation of granitic rocks (Fig. 9), the pathway of non-hybrid mafic rocks could be ascribed to fractional crystallization of mantle derived magma, that would result in WPG field for felsic rocks. But felsic rocks of KGB plot in the vicinity of the WPG/

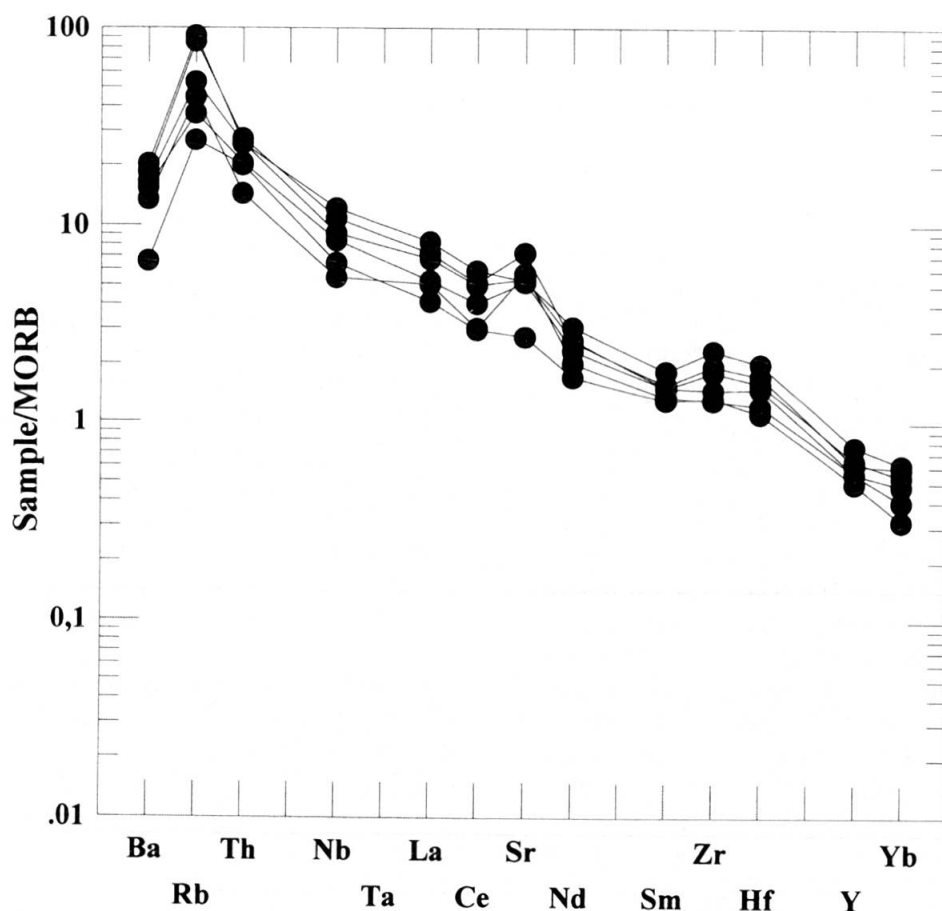


Fig. 8 MORB normalized spidergram of KGB mafic rocks.

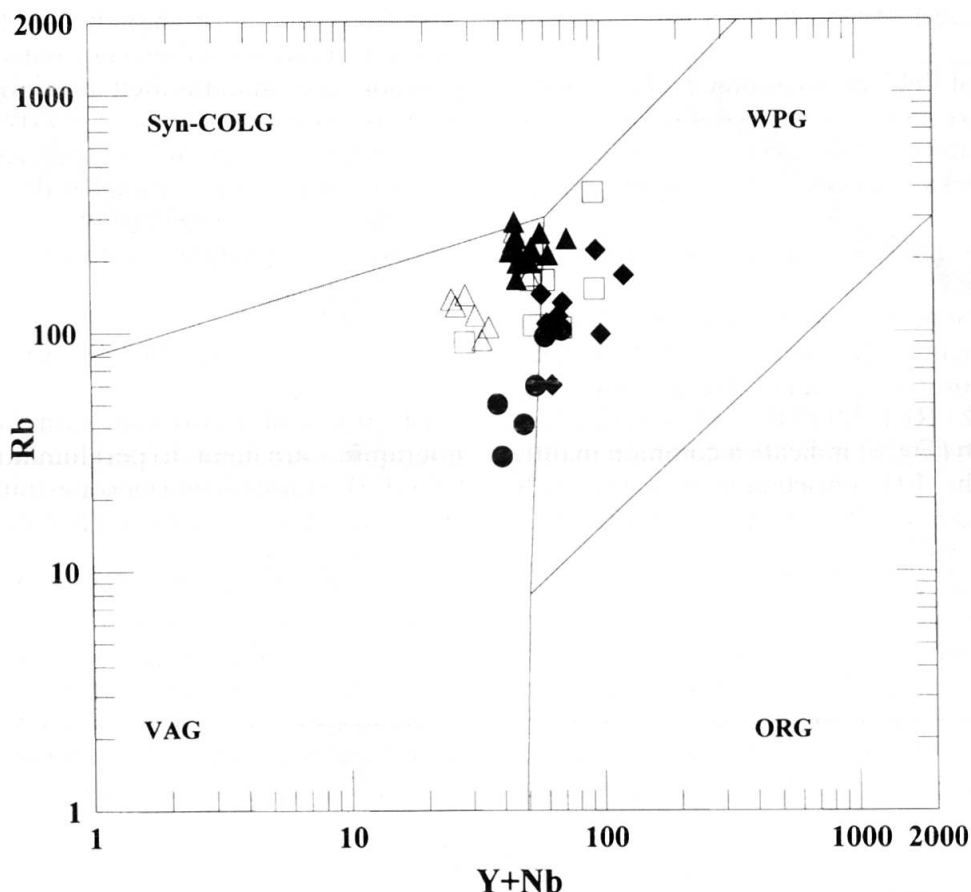


Fig. 9 Rb/Y+Nb discrimination diagram for the tectonic interpretation of granitic rocks (PEARCE et al., 1984). Symbols as in figure 2.

VAG border, partly in WPG and partly in VAG field, yielding extensive crustal contamination. ORG normalized spider diagrams with negative Ba anomaly (Fig. 10), enrichment in LIL and depletion of HFS elements, and Fe rich mica mineral chemistry suggest an early anorogenic tectonic setting (BONIN 1990, 1997; BONIN et al., 1998)

The variation diagrams of major elements vs. D.I. for syenogranite series show regular trends which can be interpreted as Liquid Lines of Descent. This indicates a leading role of fractional crystallization with some, less significant episodes of mixing. Because of the mass ratio of felsic and mafic magma (the mafic rocks represent about 20% of the whole belt), the interaction processes between the two magmas must have influenced the felsic magma as well, thus producing some hybrid syenogranite and syenite.

The field and petrographic signs of hybridization in felsic rocks are not as obvious as in mafic rocks. Hence, if we consider the behaviour of trace elements in felsic rocks, we can see that some syenogranite display important differences as higher Sr and lower Rb, Nb, Y contents. This may indicate their hybrid nature and is in good

agreement with the selective mechanism of contamination for the hybridized mafic rocks, characterized by lower Sr and higher Rb, Nb and Y contents with respect to non-hybrid enclaves.

This interpretation is also supported by the behaviour of REE patterns where the differences exist between hybrid and non-hybrid syenogranites. The depletion of REE content in hybrid syenogranite relative to non-hybrid one is in agreement with the enrichment observed in hybrid mafic rocks.

## 6. Conclusions

The rocks of the Karavanke Granitic Belt range in composition from olivine gabbro to syenogranite without a compositional gap. Field, petrographic and geochemical evidence indicate that they do not represent the result of a crystal fractionation process, nor of a simple bulk mixing process. Only some of the more mafic and some of the more felsic rocks could be consistently linked by crystal fractionation. Rocks of intermediate composition are the results of a different degree of interaction between the two end-member magmas.

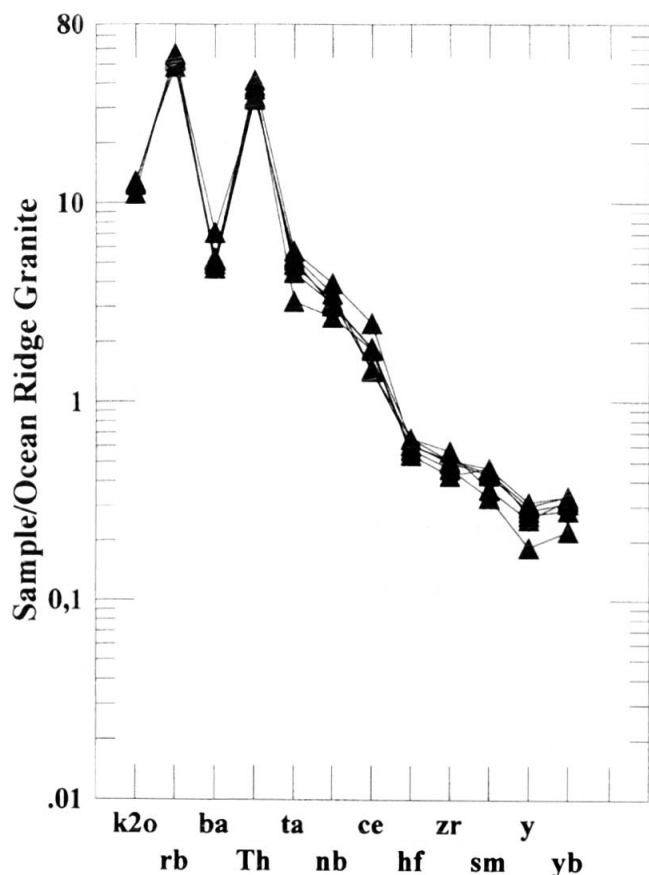


Fig. 10 ORG normalized spidergram of KGB syenogranite.

Chemical and mineralogical compositions indicate that the mafic rocks represent the mantle derived magma. Rising and fractional crystallization of mafic magma probably produced the heat necessary to trigger the melting of crustal material, which lead to the formation of the felsic magma, as suggested by initial Sr isotopic data (DOLENEC, 1994).

The highly contrasted felsic-mafic relationships and the alkaline character of rocks fit an anorogenic to post-orogenic tectonic setting according to PITCHER (1993).

Late Permian to Triassic early anorogenic A-type plutonic-volcanic complexes constitute a part of the Western Mediterranean province. The large alkaline magmatic activity of the Western Mediterranean province was related both to post-orogenic continental consolidation of the European plate, containing fragments of Gondwana accreted to Laurasia and to precursory stages of the formation of Meso-Tethys oceanic basin created from the Paleo-Tethys ocean and propagating westwards within the Gondwanaland (BONIN et al. 1987, 1998; BONIN, 1997). The Triassic (245–200 Ma) is marked by the onset of the Tethys

ocean basin spreading with the development of a large rift system and emplacement of volcanic-plutonic complexes related to strike-slip fault zones (BONIN et al., 1998).

The Triassic early anorogenic bimodal alkaline plutonic complex of the Karavanke Granitic Belt is consistent with the regime of incipient rifting suggested by BONIN et al. (1987) for the Western Mediterranean Magmatic province, thus indicating that the Triassic Karavanke Granitic Belt is also part of the same magmatic province.

#### Acknowledgements

This research was performed with the financial support of the Ministry of Science and Technology, Republic of Slovenia. Mineral chemistry was carried out at CNR-Padova, with the generous help of Prof. G. Bellieni, Dr. A. M. Fioretti and Dr. G. Cavazzini. The manuscript was improved by the comments of three reviewers, Prof. B. Bonin, Prof. J. Hernandez and Prof. A. M. Marzoli. All the financial support, help and suggestions are acknowledged and highly appreciated.

#### References

- BELLIENI, G., VISENTIN, J. E. and ZANETTIN, V. (1995): Use of chemical TAS diagram (Total Alkali Silica) for classification of plutonic rocks: Problems and suggestions. *Plinius*, 14, 49–52.
- BELLIENI, G., CAVAZZINI, G., FIORETTI, A. M., PECCERILLO, A. and ZANTEDESCHI, P. (1996): The Cima di Vila (Zinsnock) Intrusion, Eastern Alps: evidence for crustal melting, acid-mafic magma mingling and wall rock fluid effects. *Min. Petrol.*, 56, 125–146.
- BLUNDY, J. D. and SPARKS, R. S. J. (1992): Petrogenesis of mafic inclusions in granitoids of the Adamello Massif, Italy. *J. Petrol.*, 33, 5, 1039–1104.
- BONIN, B. (1990): From orogenic to anorogenic settings: evolution of granitoid suites after a major orogenesis. *Geol. J.*, 25, 261–270.
- BONIN, B. (1991): The enclaves of alkaline anorogenic granites: an overview. In: DIDIER, J. and BARBARIN, B. (eds): *Enclaves and Granite Petrology*. Elsevier, Amsterdam, 179–188.
- BONIN, B. (1997): Late Variscan magmatic evolution of the Alpine belt: an overview. In: SINHA, A. K., SASSI, F. P. and PAPANIKOLAOU, D. (eds): *Geodynamic Domains in the Alpine-Himalayan Tethys*. Oxford and IBH Publishing Pvt., New Delhi and A.A. Balkema, Rotterdam, 295–314.
- BONIN, B., PLATEVOET, B. and VIALETTE, Y. (1987): The geodynamic significance of alkaline magmatism in the western Mediterranean compared with West Africa. *Geol. J.*, 22, 361–387.
- BONIN, B., AZZOUNI-SEKKAL, A., BUSSY, F. and FERRAG, S. (1998): Alkali-calcic and alkaline post-orogenic (PO) granite magmatism: petrologic constraints and geodynamic settings. *Lithos*, 45, 45–70.
- BUSSY, F. (1990): The rapakivi texture of feldspars in a plutonic mixing environment: a dissolution-recrystallization process? *Geol. J.*, 25, 319–324.
- CASTRO, A., MORENO-VENTAS, I. and DE LA ROSA, J. D. (1990): Microgranular enclaves as indicators of hybridization processes in granitoid rocks, Hercynian Belt, Spain. *Geol. J.*, 25, 391–404.



- CLARKE, D. B. (1992): *Granitoid rocks*. Chapman & Hall, 283 pp.
- CHAPPELL, B. W. (1996): Magma mixing and the production of compositional variation within granite suites: evidence from the granites of Southeastern Australia. *J. Petrol.*, 37/3, 449–470.
- DE LA ROCHE, H., LETERRIER, J., GRANDCLAUDE, P. and MARCHAL, M. (1980): A Classification of Volcanic and Plutonic Rocks Using  $R_1/R_2$ -Diagram and Major-Element Analysis-Its Relationships With Current Nomenclature. *Chem. Geol.*, 29, 183–210.
- DIDIER, J. and BARBARIN, B. (1991): *Enclaves and Granite Petrology*. Elsevier, 625 pp.
- DOLENEC, T. (1994): Novi izotopski in radiometrični podatki o pohorskih magmatskih kamninah. *Rud. Met. Zb.*, 41, 147–152.
- EBY, N. G. (1983): The Identification of Silicate-Liquid Immiscibility Process Using Minor and Trace Elements Distribution. In: AUGUSTITHIS, S. S. (ed.): *The Significance of Trace Elements in Solving Petrogenetic Problems and Controversies*. Theophrastus Publications S. A., Athens, 27–38.
- EKLUND, O., FJÖRDÖ, S. and LINDBERG, B. (1994): Magma Mixing, the Petrogenetic Link between Anorthositic Suites and Rapakivi Granites, Åland, SW Finland. *Min. Petrol.*, 50, 3–20.
- EXNER, CH. (1971): *Geologie der Karawankenplutone Östlich Eisenkappel, Kärnten*. *Mitt. Geol. Ges.*, 64, 1–108.
- EXNER, CH. (1976): Die geologische Position der Magmatite des periadriatischen Lineamentes. *Verh. Geol. B.-A.*, 2, 3–64.
- FANINGER, E. (1974): *Geokemijske raziskave pohorskega in karavanškega tonalita*. Inštitut za geologijo, Univerze v Ljubljani, 20 pp.
- FANINGER, E. (1976): *Karavanški tonalit*. *Geologija*, 19, 153–210.
- FERRARA, G. and INNOCENTI, F. (1974): Radiometric age evidences of a Triassic Thermal Event in the Southern Alps. *Geol. Rundsch.*, 63, 572–581.
- FOURCADE, S. and ALLEGRE, C. J. (1981): Trace Elements Behaviour in Granite Genesis: A Case Study The Calc-Alkaline Plutonic Association from the Querigut Complex (Pyrenees, France). *Contrib. Mineral. Petrol.*, 76, 177–195.
- HIBBARD, M. J. (1981): The Magma Mixing Origin of Mantled Feldspars. *Contrib. Mineral. Petrol.*, 76, 158–170.
- HINTERLECHNER-RAVNIK, A. (1978): *Kontaktmetamorfne kamenine v okolici Črne pri Mežici*. *Geologija*, 21, 77–80.
- HINTERLECHNER-RAVNIK, A. (1988/89): *Ultramafični vključki v granitu Črne na Koroškem v Sloveniji*. *Geologija*, 31, 32, 403–414.
- ISAILOVIĆ, S. and MILIČEVIĆ, M. (1964): *Geološko kartiranje granita Črne na Koroškem i obodnih tvorevina*. Zavod za nuklearne sirovine, Beograd, 53 pp.
- LEAKE, B. E., WOOLEY, A. R., ARPS, C. E. S., BIRCH, W. D., GILBERT, M. C., GRICE, J. D., HAWTHORNE, F. C., KATO, A., KISCH, H. J., KRIVOVICHEV, V. G., LINTHOUT, K., LAIRD, J., MANDARINO, J. A., MARESCH, W. V., NICKEL, E. H., ROCK, N. M. S., SCHUMACHER, J. C., SMITH, D. C., STEPHENSON, N. C. N., UNGARETTI, L., WHITTAKER, E. J. W. and YOUZHI G. (1997): Nomenclature of amphiboles: Report of the Subcommittee on Amphiboles of the International Mineralogical Association, Commission on New Minerals and Mineral Names. *Am. Mineral.*, 82, 1019–1037.
- LIPPOLT, H. J. and PIDGEON, R. (1974): Isotopic Mineral Ages of a Diorite from the Eisenkappel Intrusion, Austria. *Z. Naturforsch.*, 29a, 966–968.
- MIOČ, P. (1983): *Osnovna geološka karta SFRJ 1: 100.000, tolmač za list Ravne na Koroškem (L 33–54)*. Zvezni geološki zavod, Beograd, 69 p.
- MIOČ, P. and ŽNIDARČIČ, M. (1978): *Osnovna geološka karta SFRJ 1: 100.000, tolmač za list Slovenj Gradec (L 33–55)*. Zvezni geološki zavod, Beograd, 74 p.
- MIYASHIRO, A. (1978): Nature of Alkalic Volcanic Rock Series. *Contrib. Mineral. Petrol.*, 66, 91–104.
- NAKAMURA, N. (1974): Determination of REE, Ba, Fe, Mg, Na and K in carbonaceous and ordinary chondrites. *Geochim. Cosmochim. Acta*, 38, 757–775.
- PEARCE, J. A., HARRIS, N. B. W. and TINDLE, A. G. (1984): Trace element discrimination diagrams for the tectonic interpretation of granitic rocks. *J. Petrol.*, 25, 956–983.
- PITCHER, W. S. (1993): *The Nature and Origin of Granite*. Blackie A & P, London, 321 pp.
- PLATEVOET, B. and BONIN, B. (1991): Enclaves and mafic-felsic associations in the Permian alkaline province of Corsica, France: Physical and chemical interactions between coeval magmas. In: DIDIER, J. and BARBARIN, B. (eds): *Enclaves and Granite Petrology*. Elsevier, Amsterdam, 191–204.
- POUCHOU, J. L. (1984): A new model for X-ray Microanalysis. *La recherche Aerospatiale*, 3, 167–192.
- RÄMÖ, Ö. T. and HAAPALA, I. (1995): One hundred years of Rapakivi Granite. *Min. Petrol.*, 52, 129–185.
- REID JR., J. B., EVANS, O. C. and FATES, D. G. (1983): Magma mixing in granitic rocks of the central Sierra Nevada, California. *Earth Planet. Sci. Lett.*, 66, 243–261.
- ROLLINSON, H. (1993): *Using Geochemical Data*. Longman Sc. & Tech., 352 pp.
- SALONSAARI, P. T. and HAAPALA, I. (1994): The Jaala-Itti Rapakivi Complex. An Example of Bimodal Magmatism and Hybridization in the Wiborg Rapakivi Batholith, Southeastern Finland. *Min. Petrol.*, 50, 21–35.
- SCHARBERT, S. (1975): Radiometrische Altersdaten von Intrusivgesteinen im Raum Eisenkappel (Karawanken, Kärnten). *Verh. Geol. B.-A.*, 4, 301–304.
- ŠTRUCL, I. (1970): Stratigrafske in tektonske razmere v vzhodnem delu severnih Karavank. *Geologija*, 13, 5–20.
- THORNTON, C. P. and TUTTLE, O. F. (1960): Chemistry of igneous rocks I. Differentiation Index. *Am. J. Sci.*, 258, 664–684.
- VERNON, R. H. (1991): Interpretation of microstructures of microgranitoid enclaves. In: DIDIER, J. and BARBARIN, B. (eds): *Enclaves and Granite Petrology*. Elsevier, 277–293.
- ZANETTIN, B. (1986): Classificazione chimica delle rocce vulcaniche mediante il diagramma TAS (Total Alkali-Silica). *Proposte della Sottocommissione della I.U.G.S. per la sistematica delle rocce magmatiche*. *Rend. Soc. Ital. Mineral. Petrol.*, 41/2, 193–200.
- ZORPI, M. J., COULON, C. and ORSINI, J. B. (1991): Hybridisation between felsic and mafic magmas in calc-alkaline granitoids – a case study in northern Sardinia, Italy. *Chem. Geol.*, 92, 45–87.

Manuscript received June 26, 1999; revision accepted February 13, 2001.